Figure 7. Schematic representation of the IFN signal transduction and the role of CyPA in regulating this pathway. (A) In the absence of CyP inhibitors, IFN stimulation triggers the activation of Janus-activated kinase 1, which phosphorylates STAT1 and STAT2, and translocates into the nucleus in association with ISGF3γ. Transcription of ISGs is regulated by the STAT1/STAT2/ISGF3γ complex. mRNA translation into ISG proteins is then negatively regulated by phosphorylated (activated) PKR. PKR is highly phosphorylated in HCV-infected cells. CyPA is suggested to positively regulate the phosphorylation of PKR. (B) In the presence of CyP inhibitors such as SCY-635, CyPA dissociates from PKR, which results in the impairment of the phosphorylation of PKR and releases the negative regulation of ISG protein translation.

the effect of SCY-635 on PKR phosphorylation in Huh-7 cells stimulated with poly I:C instead of infected with HCV. As shown in Figure 6A, treatment with SCY-635 reduced poly I:C–induced phosphorylation of PKR in a dose-dependent manner (in this assay, we used higher concentrations of SCY-635 [2, 4, and 8 μM] than those used in the assay with HCV-infected cells) (Figure 6A). The SG formation triggered by poly I:C via phosphorylated PKR was consistently inhibited by SCY-635 (Figure 6B). These data suggest that the modulation of PKR by SCY-635 was not limited to cells infected with HCV, consistent with the molecular interaction of CyPA with PKR in uninfected cells (Figure 4, *lane 6*). Arsenite is known to induce SG formation but through a mechanism independent of PKR.[38] As shown in Figure 6B, SCY-635 did not affect the formation of SGs induced by arsenite (Figure 6B), further suggesting that the functional regulation by CyPA is specific to PKR. Therefore, CyPA was suggested to be a positive regulator of PKR.

Discussion

In this study, we showed that CyP inhibitors restored IFN-induced ISG protein production through impairment of PKR phosphorylation. CyPA was specifically required for the regulation of PKR phosphorylation and the formation of stress granules. These results suggest that CyP inhibitors potentiate the anti-HCV effect of IFN in HCV-infected cells. It was reported that the clinical anti-HCV activity of CyP inhibitors (when given as monotherapy) was possibly influenced by IL28B genotypes, as is the case with IFN-based treatment,[23,24] suggesting a cross talk between CyP inhibitors and IFN pathway. In a separate clinical study in difficult to treat patients with IL28B genotype CT or TT,

therapy with a CyP inhibitor in combination with IFN resulted in improved rates of sustained virologic response as compared with patients treated with IFN alone.[39] Our study clearly presents a molecular basis for this clinical observation: at least some portion of the anti-HCV activity of CyP inhibitors is mediated by the potentiation of IFN action.

The anti-HCV activity of CyP inhibitors reported to date is attributed mainly to direct inhibition of the function or formation of the RNA replication complex.[13,17,40–42] Huh-7, Huh-7.5, and Huh-7.5.1 cells that are typically used for HCV cell culture studies are partly or fully deficient for IFN induction, and produce little IFN alfa, although the IFN response to ISG induction is active.[43,44] Therefore, results obtained in these cell lines would primarily evaluate direct effects on HCV replication with little IFN-alfa production. In contrast, under conditions of functional IFN-induction pathways, such as in HCV-infected patients, the modulatory effect of CyP inhibitors on IFN signaling pathway might play a more relevant role in achieving anti-HCV activity. In support of this, it has been reported that combination treatment of CyP inhibitors with ectopic IFN alfa exhibited a synergistic anti-HCV activity both in cell culture and in the clinical setting.[16,45–47] We also showed that a CyP inhibitor augmented the anti-HCV activity of IFN alfa (Figure 2C). HCV-infected patients treated with SCY-635 alone showed up-regulation of IFN alfa and oligoadenylate synthetase proteins, both of which are representative ISGs, which corresponded with SCY-635 concentrations in serum.[23] Clinically, ectopically administered IFN induces substantial side effects, and IFN-free therapy has been greatly demanded.[4] Interestingly, the induction of endogenous IFN observed with SCY-635 monotherapy did not produce any of the serious side effects typically observed with IFN-based

therapy.[23] Our study raises the possibility that CyP inhibitors can be used as a replacement for exogenous IFN in the treatment of HCV. This is of particular importance because it has been shown that treatment with direct-acting antivirals alone might not be sufficient to cure HCV infection across all HCV genotypes, and that addition of IFN can increase the rates of sustained virologic response.[1,48]

Although it has been reported that HCV E2 and NS5A inhibited PKR activity,[49,50] PKR was highly phosphorylated in HCV-infected cells (Figure 2), as reported previously,[29,43] possibly through stimulation by the 5′-untranslated region of HCV RNA.[51] Activated PKR suppressed host protein translation, including ISGs, without affecting HCV internal ribosome entry site–dependent translation.[29,43] Garaigorta et al further reported that a knockdown of endogenous PKR restored ISG protein induction by IFN alfa in HCV-infected cells to augment the anti-HCV effect of IFN alfa. They speculate that inhibitors blocking PKR activation can be therapeutic agents to eliminate HCV from infected cells.[29] Consistent with this idea, our study revealed that CyP inhibitors suppressed PKR phosphorylation and restored ISG protein induction at the translational level. A clinical study with SCY-635 monotherapy demonstrated an increase in ISG protein production in HCV-infected patients treated with SCY-635.[23] These results are likely to support the proposed mechanism of the CyP inhibitors on the translational regulation of ISG proteins (Figure 7). CyP inhibitors can reverse the IFN-resistant mechanism in HCV-infected cells mediated by a reduced response of ISG protein induction.

In general, through the recognition of double-stranded RNA, PKR is dimerized and then autophosphorylated at T446.[28] The phosphorylated PKR interacts with and phosphorylates the downstream target eIF2α to negatively regulate the translation of proteins. We hypothesize that CyPA is acting as a molecular chaperone and possibly regulates one or more steps in this activation process of PKR, including ligand recognition, dimerization, and phosphorylation. Additional analyses are required to address which step in PKR activation is regulated by CyPA. However, this study indicates that the double-stranded RNA activation mechanism of PKR is a target for CyP inhibitors, which show significant clinical effects in HCV-infected patients. Our results further suggest that PKR can serve as a target for the development of anti-HCV agents.

Supplementary Material

Note: To access the supplementary material accompanying this article, visit the online version of *Gastroenterology* at www.gastrojournal.org, and at http://dx.doi.org/10.1053/j.gastro.2014.04.035.

References

1. Liang TJ, Ghany MG. Current and future therapies for hepatitis C virus infection. N Engl J Med 2013; 368:1907–1917.

2. Liang TJ, Heller T. Pathogenesis of hepatitis C-associated hepatocellular carcinoma. Gastroenterology 2004; 127(Suppl 1):S62–S71.

3. Pawlotsky JM. Treatment failure and resistance with direct-acting antiviral drugs against hepatitis C virus. Hepatology 2011;53:1742–1751.

4. Pawlotsky JM. The science of direct-acting antiviral and host-targeted agent therapy. Antivir Ther 2012; 17:1109–1117.

5. Pawlotsky JM. Treatment of chronic hepatitis C: current and future. Curr Top Microbiol Immunol 2013; 369:321–342.

6. Thimme R, Binder M, Bartenschlager R. Failure of innate and adaptive immune responses in controlling hepatitis C virus infection. FEMS Microbiol Rev 2012; 36:663–683.

7. Aghemo A, De Francesco R. New horizons in hepatitis C antiviral therapy with direct-acting antivirals. Hepatology 2013;58:428–438.

8. Bergmann JF, De Knegt RJ, Janssen HL. What is on the horizon for treatment of chronic hepatitis C? Minerva Med 2008;99:569–582.

9. Shimakami T, Lanford RE, Lemon SM, Hepatitis C. recent successes and continuing challenges in the development of improved treatment modalities. Curr Opin Pharmacol 2009;9:537–544.

10. Wedemeyer H. Hepatitis C in 2012: on the fast track towards IFN-free therapy for hepatitis C? Nat Rev Gastroenterol Hepatol 2013;10:76–78.

11. Zeisel MB, Lupberger J, Fofana I, et al. Host-targeting agents for prevention and treatment of chronic hepatitis C—perspectives and challenges. J Hepatol 2013; 58:375–384.

12. Buhler S, Bartenschlager R. New targets for antiviral therapy of chronic hepatitis C. Liver Int 2012;32(Suppl 1):9–16.

13. Gallay PA. Cyclophilin inhibitors. Clin Liver Dis 2009; 13:403–417.

14. Watashi K, Shimotohno K. Cyclophilin and viruses: cyclophilin as a cofactor for viral infection and possible anti-viral target. Drug Target Insights 2007;2:9–18.

15. El-Farrash MA, Aly HH, Watashi K, et al. In vitro infection of immortalized primary hepatocytes by HCV genotype 4a and inhibition of virus replication by cyclosporin. Microbiol Immunol 2007;51:127–133.

16. Goto K, Watashi K, Murata T, et al. Evaluation of the anti-hepatitis C virus effects of cyclophilin inhibitors, cyclosporin A, and NIM811. Biochem Biophys Res Commun 2006;343:879–884.

17. **Ishii N**, **Watashi K**, Hishiki T, et al. Diverse effects of cyclosporine on hepatitis C virus strain replication. J Virol 2006;80:4510–4520.

18. Watashi K, Hijikata M, Hosaka M, et al. Cyclosporin A suppresses replication of hepatitis C virus genome in cultured hepatocytes. Hepatology 2003;38: 1282–1288.

19. Yang F, Robotham JM, Nelson HB, et al. Cyclophilin A is an essential cofactor for hepatitis C virus infection and the principal mediator of cyclosporine resistance in vitro. J Virol 2008;82:5269–5278.

20. Chatterji U, Bobardt M, Selvarajah S, et al. The isomerase active site of cyclophilin A is critical for hepatitis C virus replication. J Biol Chem 2009;284: 16998–17005.

21. Goto K, Watashi K, Inoue D, et al. Identification of cellular and viral factors related to anti-hepatitis C virus activity of cyclophilin inhibitor. Cancer Sci 2009;100: 1943–1950.

22. Kaul A, Stauffer S, Berger C, et al. Essential role of cyclophilin A for hepatitis C virus replication and virus production and possible link to polyprotein cleavage kinetics. PLoS Pathog 2009;5:e1000546.

23. Hopkins S, DiMassimo B, Rusnak P, et al. The cyclophilin inhibitor SCY-635 suppresses viral replication and induces endogenous interferons in patients with chronic HCV genotype 1 infection. J Hepatol 2012;57:47–54.

24. Kaiser S, Gallay P, Bobardt M, et al. Down-regulation of interferon-stimulated genes after alisporivir interferon-free treatment suggests a unique antiviral mechanism of action for alisporivir, a cyclophilin inhibitor. J Hepatol 2013;58:S342.

25. Lemon SM. Induction and evasion of innate antiviral responses by hepatitis C virus. J Biol Chem 2010;285: 22741–22747.

26. Saito T, Gale M Jr. Regulation of innate immunity against hepatitis C virus infection. Hepatol Res 2008; 38:115–122.

27. Saito T, Owen DM, Jiang F, et al. Innate immunity induced by composition-dependent RIG-I recognition of hepatitis C virus RNA. Nature 2008;454:523–527.

28. Dabo S, Meurs EF. dsRNA-dependent protein kinase PKR and its role in stress, signaling and HCV infection. Viruses 2012;4:2598–2635.

29. Garaigorta U, Chisari FV. Hepatitis C virus blocks interferon effector function by inducing protein kinase R phosphorylation. Cell Host Microbe 2009;6:513–522.

30. Garaigorta U, Heim MH, Boyd B, et al. Hepatitis C virus (HCV) induces formation of stress granules whose proteins regulate HCV RNA replication and virus assembly and egress. J Virol 2012;86:11043–11056.

31. Ruggieri A, Dazert E, Metz P, et al. Dynamic oscillation of translation and stress granule formation mark the cellular response to virus infection. Cell Host Microbe 2012; 12:71–85.

32. Heim MH. Interferons and hepatitis C virus. Swiss Med Wkly 2012;142:w13586.

33. Horner SM, Gale M Jr. Intracellular innate immune cascades and interferon defenses that control hepatitis C virus. J Interferon Cytokine Res 2009;29:489–498.

34. Lin K, Perni RB, Kwong AD, et al. VX-950, a novel hepatitis C virus (HCV) NS3-4A protease inhibitor, exhibits potent antiviral activities in HCv replicon cells. Antimicrob Agents Chemother 2006;50:1813–1822.

35. Brazin KN, Mallis RJ, Fulton DB, et al. Regulation of the tyrosine kinase Itk by the peptidyl-prolyl isomerase cyclophilin A. Proc Natl Acad Sci U S A 2002;99: 1899–1904.

36. Tata JR. Signalling through nuclear receptors. Nat Rev Mol Cell Biol 2002;3:702–710.

37. Vyssokikh MY, Katz A, Rueck A, et al. Adenine nucleotide translocator isoforms 1 and 2 are differently distributed in the mitochondrial inner membrane and have distinct affinities to cyclophilin D. Biochem J 2001; 358:349–358.

38. **Ghisolfi L, Dutt S**, McConkey ME, et al. Stress granules contribute to alpha-globin homeostasis in differentiating erythroid cells. Biochem Biophys Res Commun 2012; 420:768–774.

39. Muir AJ, Rodriguez-Torres M, Borroto-Esoda K, et al. Short duration treatment with SCY-635 restores sensitivity to Peg-IFN/RBV in difficult to treat, IL28B TT/CT, HCV genotype 1 patients. Hepatology 2012; 56:191A.

40. Hanoulle X, Badillo A, Wieruszeski JM, et al. Hepatitis C virus NS5A protein is a substrate for the peptidyl-prolyl cis/trans isomerase activity of cyclophilins A and B. J Biol Chem 2009;284:13589–13601.

41. Hopkins S, Bobardt M, Chatterji U, et al. The cyclophilin inhibitor SCY-635 disrupts hepatitis C virus NS5A-cyclophilin A complexes. Antimicrob Agents Chemother 2012;56:3888–3897.

42. Yang F, Robotham JM, Grise H, et al. A major determinant of cyclophilin dependence and cyclosporine susceptibility of hepatitis C virus identified by a genetic approach. PLoS Pathog 2010;6:e1001118.

43. Arnaud N, Dabo S, Maillard P, et al. Hepatitis C virus controls interferon production through PKR activation. PLoS One 2010;5:e10575.

44. Sumpter R Jr, Loo YM, Foy E, et al. Regulating intracellular antiviral defense and permissiveness to hepatitis C virus RNA replication through a cellular RNA helicase, RIG-I. J Virol 2005;79:2689–2699.

45. Ma S, Boerner JE, TiongYip C, et al. NIM811, a cyclophilin inhibitor, exhibits potent in vitro activity against hepatitis C virus alone or in combination with alpha interferon. Antimicrob Agents Chemother 2006;50: 2976–2982.

46. Flisiak R, Feinman SV, Jablkowski M, et al. The cyclophilin inhibitor Debio 025 combined with PEG IFNalpha2a significantly reduces viral load in treatment-naive hepatitis C patients. Hepatology 2009; 49:1460–1468.

47. Inoue K, Sekiyama K, Yamada M, et al. Combined interferon alpha2b and cyclosporin A in the treatment of chronic hepatitis C: controlled trial. J Gastroenterol 2003; 38:567–572.

48. Lawitz E, Mangia A, Wyles D, et al. Sofosbuvir for previously untreated chronic hepatitis C infection. N Engl J Med 2013;368:1878–1887.

49. Taylor DR, Shi ST, Romano PR, et al. Inhibition of the interferon-inducible protein kinase PKR by HCV E2 protein. Science 1999;285:107–110.

50. Gale M Jr, Blakely CM, Kwieciszewski B, et al. Control of PKR protein kinase by hepatitis C virus nonstructural 5A protein: molecular mechanisms of kinase regulation. Mol Cell Biol 1998;18:5208–5218.

51. Toroney R, Nallagatla SR, Boyer JA, et al. Regulation of PKR by HCV IRES RNA: importance of domain II and NS5A. J Mol Biol 2010;400:393–412.

BASIC AND TRANSLATIONAL LIVER

BASIC AND
TRANSLATIONAL LIVER

Involvement of Hepatitis C Virus NS5A Hyperphosphorylation Mediated by Casein Kinase I-α in Infectious Virus Production

Takahiro Masaki,[a,e] Satoko Matsunaga,[b] Hirotaka Takahashi,[b] Kenji Nakashima,[d] Yayoi Kimura,[c] Masahiko Ito,[d] Mami Matsuda,[a] Asako Murayama,[a] Takanobu Kato,[a] Hisashi Hirano,[c] Yaeta Endo,[b] Stanley M. Lemon,[e,f,g] Takaji Wakita,[a] Tatsuya Sawasaki,[b] Tetsuro Suzuki[d]

Department of Virology II, National Institute of Infectious Diseases, Toyama, Shinjuku-ku, Tokyo, Japan[a]; Proteo-Science Center, Ehime University, Matsuyama, Ehime, Japan[b]; Graduate School of Medical Life Science and Advanced Medical Research Center, Yokohama City University, Fukuura, Kanazawa-ku, Yokohama, Japan[c]; Department of Infectious Diseases, Hamamatsu University School of Medicine, Handayama, Higashi-ku, Hamamatsu, Japan[d]; Lineberger Comprehensive Cancer Center,[e] Division of Infectious Diseases, Department of Medicine,[f] and Department of Microbiology and Immunology,[g] The University of North Carolina at Chapel Hill, Chapel Hill, North Carolina, USA

ABSTRACT

Nonstructural protein 5A (NS5A) of hepatitis C virus (HCV) possesses multiple functions in the viral life cycle. NS5A is a phosphoprotein that exists in hyperphosphorylated and basally phosphorylated forms. Although the phosphorylation status of NS5A is considered to have a significant impact on its function, the mechanistic details regulating NS5A phosphorylation, as well as its exact roles in the HCV life cycle, are still poorly understood. In this study, we screened 404 human protein kinases via *in vitro* binding and phosphorylation assays, followed by RNA interference-mediated gene silencing in an HCV cell culture system. Casein kinase I-α (CKI-α) was identified as an NS5A-associated kinase involved in NS5A hyperphosphorylation and infectious virus production. Subcellular fractionation and immunofluorescence confocal microscopy analyses showed that CKI-α-mediated hyperphosphorylation of NS5A contributes to the recruitment of NS5A to low-density membrane structures around lipid droplets (LDs) and facilitates its interaction with core protein and the viral assembly. Phospho-proteomic analysis of NS5A with or without CKI-α depletion identified peptide fragments that corresponded to the region located within the low-complexity sequence I, which is important for CKI-α-mediated NS5A hyperphosphorylation. This region contains eight serine residues that are highly conserved among HCV isolates, and subsequent mutagenesis analysis demonstrated that serine residues at amino acids 225 and 232 in NS5A (genotype 2a) may be involved in NS5A hyperphosphorylation and hyperphosphorylation-dependent regulation of virion production. These findings provide insight concerning the functional role of NS5A phosphorylation as a regulatory switch that modulates its multiple functions in the HCV life cycle.

IMPORTANCE

Mechanisms regulating NS5A phosphorylation and its exact function in the HCV life cycle have not been clearly defined. By using a high-throughput screening system targeting host protein kinases, we identified CKI-α as an NS5A-associated kinase involved in NS5A hyperphosphorylation and the production of infectious virus. Our results suggest that the impact of CKI-α in the HCV life cycle is more profound on virion assembly than viral replication via mediation of NS5A hyperphosphorylation. CKI-α-dependent hyperphosphorylation of NS5A plays a role in recruiting NS5A to low-density membrane structures around LDs and facilitating its interaction with the core for new virus particle formation. By using proteomic approach, we identified the region within the low-complexity sequence I of NS5A that is involved in NS5A hyperphosphorylation and hyperphosphorylation-dependent regulation of infectious virus production. These findings will provide novel mechanistic insights into the roles of NS5A-associated kinases and NS5A phosphorylation in the HCV life cycle.

H epatitis C virus (HCV) is a major causative agent of liver-related morbidity and mortality worldwide and represents a global public health problem (1). An estimated 130 million individuals are chronically infected with HCV worldwide, and the treatment of HCV infection imposes a large economic and societal burden (2). HCV is an enveloped virus with a positive-sense, single-stranded RNA genome in the *Hepacivirus* genus within the *Flaviviridae* family (3). The approximately 9.6-kb genome is translated into a single polypeptide of approximately 3,000 amino acids (aa), which is cleaved by cellular and viral proteases to produce the structural proteins (core, E1, E2, and p7) and nonstructural (NS) proteins (NS2, NS3, NS4A, NS4B, NS5A, and NS5B) (4). NS3 to NS5B are sufficient for RNA replication in cell culture (5). NS5B is an RNA-dependent RNA polymerase (RdRp), and NS3 functions as both an RNA helicase and a serine protease (4).

NS4A is the cofactor of the NS3 protease, and the NS3-NS4A complex is required for viral precursor processing (4). NS4B induces the formation of a specialized membrane compartment, a sort of membranous web where viral RNA replication may take

July 2014 Volume 88 Number 13
Journal of Virology p. 7541–7555
jvi.asm.org 7541

place (6). NS5A is essential for both viral RNA replication and virion assembly (7–9).

NS5A is an RNA binding protein and exists as a component of the replicase complex (10–13). NS5A is phosphorylated on multiple serine and threonine residues and can be found in hyperphosphorylated (p58) and basally phosphorylated (p56) forms (14–16). Although the distinct mechanisms for generating p56 and p58 forms are still unclear, it has been reported that two regions located around the center and near the C-terminal regions of NS5A are required for basal phosphorylation, while hyperphosphorylation primarily targets serine residues located within low-complexity sequence I (LCS I), which is the linker between domains I and II (15, 17–19). Several phosphorylation sites have been mapped in NS5A by using recombinantly expressed protein and NS5A extracted from cells harboring subgenomic replicons (20–23).

NS5A phosphorylation plays roles in the regulation of viral RNA replication and virion assembly. Some of the cell culture-adaptive mutations in NS4B and NS5A, which reduce NS5A hyperphosphorylation, have been found to confer efficient replication of genotype 1 replicons in Huh-7 cells (17, 18). Similarly, suppression of NS5A hyperphosphorylation through either the use of kinase inhibitors or mutagenesis allows higher RNA replication in non-culture-adapted replicons (18, 24). In contrast, HCV RNA replication is inhibited after treatment of cells carrying adapted replicons with the same kinase inhibitor (24). The C-terminal domain III of NS5A is not essential for viral RNA replication, but it is important for the production of infectious virus. Alanine replacements of the serine cluster in this domain impair NS5A phosphorylation, leading to a decrease in NS5A-core protein interaction, perturbation of the subcellular distribution of NS5A, and disruption of virion production (7–9).

A number of protein kinases have been identified as having the ability to phosphorylate NS5A based on comprehensive screening by using an RNA interference (RNAi) library, recombinantly expressed kinases, and kinase inhibitors (25–28). Among them, casein kinase I-α (CKI-α) and Polo-like kinase 1 (Plk1) have been shown to play roles in viral RNA replication (25, 27). Although silencing of CKI-α inhibits the replication of the genotype 1b subgenomic replicon containing an adaptive mutation (27), its effect on infectious virus production has not been studied to date. Casein kinase II (CKII) has been identified as a positive regulator of virus production via studies with chemical inhibitors and small interfering RNA (siRNA) (9). However, the functional roles of NS5A phosphorylation by its associated kinases in regulation of the viral life cycle are not yet fully understood.

To identify NS5A-associated kinases involved in the HCV life cycle, we developed an *in vitro*, high-throughput screening system for analyzing protein-protein interactions. Using this system followed by *in vitro* phosphorylation assays, we screened human protein kinases on a kinome-wide scale and identified several NS5A-associated kinases. siRNA experiments showed that silencing of CKI-α leads to the most marked inhibition of infectious virus production among the candidate kinases. Here, we report a novel function of CKI-α in the viral life cycle. It is more likely that CKI-α has a more profound impact on virion assembly than on viral replication through hyperphosphorylation of NS5A. Hyperphosphorylated NS5A was predominantly localized in low-density membrane structures around lipid droplets (LDs), in which NS5A interacts with the core for virion assembly, while reduction of

NS5A hyperphosphorylation by siRNA targeting CKI-α led to a decrease in NS5A abundance in the low-density membrane structures. The present study provides important insights into the regulatory roles of NS5A-associated kinases and NS5A phosphorylation in the viral life cycle, especially as a molecular switch governing the transition between viral replication and virion assembly.

MATERIALS AND METHODS

Plasmids. Plasmids pJFH1 and pSGR-JFH1/Luc were generated as previously described (29, 30). The JFH-1-based *Gaussia princeps* luciferase (GLuc) reporter construct, which encodes GLuc followed by the foot-and-mouth disease virus (FMDV) 2A protein between p7 and NS2, was generated in a manner similar to the description in a previous report (31). A 1,042-bp double-stranded DNA fragment containing GLuc (32) and FMDV 2A (33) sequences flanked by BsaI and NotI sites at its ends was synthesized and then inserted into the corresponding sites of pJFH1. Related constructs containing serine-to-alanine or serine-to-aspartic acid mutations in NS5A were generated using oligonucleotide-directed mutagenesis techniques. To construct pCAG-CKI-α, the full-length CKI-α-coding sequence was amplified by PCR using cDNAs prepared from Huh-7 cells. The resulting PCR product was then inserted into the multiple-cloning site of pCAGGS (34). pCAG-CKI-α/m6, which contains six silent point mutations that ablate the binding of CKI-α siRNA but maintain the wild-type amino acid sequence of CKI-α, was generated by oligonucleotide-directed mutagenesis of pCAG-CKI-α. All PCR products were confirmed by automated nucleotide sequencing with an ABI Prism 7000 sequence detection system (Life Technologies, Carlsbad, CA).

Cells. The human hepatoma cell line Huh-7, its derivative cell lines Huh7.5.1 (35) (a gift from Francis V. Chisari, The Scripps Research Institute) and Huh7–25 (36), and the human embryonic kidney cell line 293T used to generate HCV pseudoparticles (HCVpp), were maintained in Dulbecco modified Eagle medium (DMEM) supplemented with nonessential amino acids, 100 U of penicillin/ml, 100 μg of streptomycin/ml, and 10% fetal bovine serum (FBS) at 37°C in a 5% CO_2 incubator. SGR-JFH1/LucNeo cells, which harbor a genotype 2a subgenomic replicon carrying a firefly luciferase reporter gene fused to the neomycin phosphotransferase gene of pSGR-JFH1 (37), and LucNeo#2 cells, which harbor a genotype 1b subgenomic replicon carrying a firefly luciferase/neomycin phosphotransferase fusion reporter gene (38, 39) (a gift from Koichi Watashi, National Institute of Infectious Diseases, and Kunitada Shimotohno, National Center for Global Health and Medicine), were cultured in the above medium supplemented with 300 μg/ml G418.

Antibodies. Mouse monoclonal antibody against core protein (2H9) was generated as described previously (30). Anti-NS5A mouse monoclonal antibody (9E10) was a kind gift from Charles M. Rice (The Rockefeller University), and anti-NS5A rabbit polyclonal antibody (TB0705#1) was developed by immunization with the recombinant NS5A protein (8, 40). For detection of cellular proteins, the following antibodies were used: mouse monoclonal antibodies directed against Plk1 (Life Technologies) and glyceraldehyde 3-phosphate dehydrogenase (GAPDH; Millipore, Temecula, CA); rabbit polyclonal antibodies detecting CKI-α (Santa Cruz Biotechnology, Dallas, TX), CKI-ε (Santa Cruz Biotechnology), cyclinc AMP (cAMP)-dependent protein kinase catalytic subunit β (PKACβ; Santa Cruz Biotechnology), phosphatidylinositol 4-kinase IIIα (PI4K-IIIα; Cell Signaling Technology, Danvers, MA), claudin-1 (CLDN1; Life Technologies), calnexin (Enzo Life Sciences, Farmingdale, NY), and GM130 (Sigma-Aldrich, St. Louis, MO); and goat polyclonal antibodies specific for CKII-α′ (Santa Cruz Biotechnology) and apolipoprotein E (ApoE; Millipore). Fluorescence-conjugated secondary antibodies, including Alexa Fluor 488 goat anti-mouse IgG1 and Alexa Fluor 568 goat anti-mouse IgG2a, were purchased from Life Technologies. Horseradish peroxidase (HRP)-conjugated secondary antibodies were from Cell Signaling Technology.

– 324 –

Protein kinase library and cell-free protein synthesis. The construction and identity of the 404 cDNAs encoding human protein kinases used in this study were previously described (41). *In vitro* transcription and cell-free protein synthesis were performed as previously reported (42, 43). Briefly, DNA templates containing a biotin-ligating sequence were amplified by split-primer PCR with kinase cDNAs and corresponding primers and then used for protein synthesis with a fully automated protein synthesizer, a GenDecoder (CellFree Sciences, Ehima, Japan). For synthesis of FLAG-tagged full-length NS5A and domain III proteins derived from the JFH-1 isolate, DNA templates containing a FLAG sequence were generated from the NS5A expression plasmid (8) by split-primer PCR and used with a wheat germ expression kit (CellFree Sciences) according to the manufacturer's instructions.

Amplified luminescent proximity homogeneous assay (AlphaScreen). FLAG-tagged NS5A proteins were mixed with biotinylated kinases in 15 μl of reaction buffer (20 mM Tris-HCl [pH 7.6], 5 mM $MgCl_2$, 1 mM dithiothreitol, and 1 mg/ml bovine serum albumin) in the wells of 384-well OptiPlates (PerkinElmer, Waltham, MA) and incubated at 26°C for 1 h. The mixture was then added to the detection mixture containing 0.1 μl protein A-conjugated acceptor beads (PerkinElmer), 0.1 μl streptavidin-coated donor beads (PerkinElmer), and 5 μg/ml of the anti-FLAG M2 antibody, followed by incubation at 26°C for 1 h. AlphaScreen signals from the mixture were detected using an EnVision device (PerkinElmer) with the AlphaScreen signal detection program.

In vitro phosphorylation assay. To obtain purified kinases used for *in vitro* phosphorylation assays, DNA templates containing a glutathione S-transferase (GST)–tobacco etch virus (TEV) sequence were generated by split-primer PCR with kinase cDNAs and corresponding primers and used in a cell-free production system with the wheat germ expression kit as described above. The GST-fusion recombinant proteins were purified on glutathione-Sepharose 4B (GE Healthcare, Buckinghamshire, United Kingdom) and then eluted in 40 μl of phosphate-buffered saline (PBS) containing 5 U of AcTEV protease (Life Technologies) in order to cleave the GST tag from the protein. Biotinylated NS5A proteins were synthesized from DNA templates by using the cell-free BirA system (44). Biotinylated NS5A proteins (40 μl) were coupled on 15 μl of streptavidin Magnesphere Paramagnetics particles (Promega, Madison, WI) and were dephosphorylated by using 10 U of lambda protein phosphatase (New England BioLabs, Ipswich, MA). After washing three times, protein-coupled beads were incubated with 1 μl of purified recombinant kinases at 37°C for 30 min in 15 μl kinase buffer (50 mM Tris-HCl [pH 7.6], 500 mM potassium acetate, 50 mM $MgCl_2$, and 0.5 mM dithiothreitol) containing 1 μCi of [γ-^{32}P]ATP. After the reaction, the beads were washed twice with PBS and then boiled in sample buffer and separated by SDS-PAGE. Phosphorylated NS5A proteins were visualized via autoradiography, and the relative kinase activity of each kinase was determined by normalizing the band intensity of NS5A to that of NS5A incubated with dihydrofolate reductase (DHFR). The band intensities were quantified using Image J software.

Preparation of viral stocks and virus infections. Cell culture-derived infectious HCV particles (HCVcc) were prepared as described previously (30, 36). HCVpp consisting of HCV envelope glycoproteins, the murine leukemia virus Gag-Pol core proteins, and the luciferase transfer vector and pseudoparticles with the vesiclar stomatitis virus G glycoprotein (VSV-Gpp) were generated in accordance with methods described previously (36, 45). Cells seeded onto 24-well plates were transfected with siRNA and/or plasmid DNA as described below and infected with HCVcc for 4 h at a multiplicity of infection (MOI) of 0.5 to 5 or with diluted supernatant containing HCVpp or VSV-Gpp for 3 h. After infection, the cells were washed with PBS and incubated in fresh complete growth medium for 72 h at 37°C until harvest.

siRNA and plasmid DNA transfections. siRNAs were purchased from Sigma-Aldrich. The sequences were as follows: CKI-α, 5'-GGCUAAAGG CUGCAACAAAdTdT-3' and 5'-UUUGUUGCAGCCUUUAGCCdTdT-3'; CKI-γ1, 5'-GAGAUGAUUUGGAAGCCCUdTdT-3' and 5'-AGGGC

UUCCAAAUCAUCUCdTdT-3'; CKI-γ2, 5'-GCGAGAACUUCCCAGA GGAdTdT-3' and 5'-UCCUCUGGGAAGUUCUCGCdTdT-3'; CKI-γ3, 5'-CUUACAGGAACAGCUAGAUdTdT-3' and 5'-AUCUAGCUGU UCCUGUAAGdTdT-3'; CKI-ε, 5'-GCGACUACAACGUGAUGGUdTd T-3' and 5'-ACCAUCACGUUGUAGUCGCdTdT-3'; CKII-α', 5'-CCU AGAUCUUCUGGACAAAdTdT-3' and 5'-UUUGUCCAGAAGAUCU AGGdTdT-3'; PKACβ, 5'-CAAAUAGAGCAUACUUUGAdTdT-3' and 5'-UCAAAGUAUGCUCUAUUUGdTdT-3'; Plk1, 5'-GUCUCAAGGC CUCCUAAUAdTdT-3' and 5'-UAUUAGGAGGCCUUGAGACdTdT-3'; TSSK2, 5'-CACCUACUGACUUUGUGGAdTdT-3' and 5'-UCCAC AAAGUCAGUAGGUGdTdT-3'; ApoE, 5'-GGAGUUGAAGGCCUACA AAdTdT-3' and 5'-UUUGUAGGCCUUCAACUCCdTdT-3'; CLDN1, 5'-CAGUCAAUGCCAGGUACGAdTdT-3' and 5'-UCGUACCUGGCA UUGACUGdTdT-3'; PI4K-IIIα, 5'-CCCUAAAGGCGACGAGAGAdTd T-3' and 5'-UCUCUCGUCGCCUUUAGGGdTdT-3'. The Mission siRNA universal negative control (Sigma-Aldrich), which is designed to have no homology to known gene sequences, was used as a negative control. Silencer Cy3-labeled GAPDH siRNA (Life Technologies) was used to confirm siRNA delivery efficiency. Basically, 10 nM siRNAs were transfected into cells by using Lipofectamine RNAiMax (Life Technologies) according to the manufacturer's recommended procedures. Plk1 siRNA was transfected at 5 nM because of its cytotoxic effect. Plasmid DNA transfection was carried out by using TransIT-LT1 transfection reagent (Mirus, Madison, WI) according to the manufacturer's protocol. For cotransfection of siRNA and plasmid DNA, 6 pmol of siRNA and 200 ng of plasmid DNA were transfected into Huh7.5.1 cells seeded onto a 24-well cell culture plate by using Lipofectamine 2000 (Life Technologies) according to the manufacturer's instructions.

RNA synthesis and electroporation. HCV RNA synthesis and electroporation were basically performed as described previously (8). In the context of coelectroporation of siRNA and an *in vitro*-synthesized subgenomic reporter replicon, or full-length HCV RNA, a total of 3 × 10⁶ to 5 × 10⁶ Huh-7 cells were electroporated with 120 pmol siRNA and 3 μg SGR-JFH1/Luc RNA or 5 μg JFH-1 RNA at 260 V and 950 μF. After electroporation, the cells were immediately transferred onto 24-well or 6-well culture plates or 10-cm cell culture dishes.

Luciferase assay. Cells harboring a subgenomic reporter replicon and HCVpp-infected cells were lysed in passive lysis buffer (Promega). The luciferase activity was determined using a luciferase assay system (Promega) as previously described (46). Secreted GLuc activity was measured in 25-μl aliquots of cell culture supernatants by using the BioLux *Gaussia* luciferase assay kit (New England BioLabs) according to the manufacturer's recommended protocol. The luminescence signal was measured on an Infinite M200 microplate reader (Tecan, Männedorf, Switzerland).

Quantification of HCV core. HCV core protein in cell lysates and culture supernatants was quantified by using a highly sensitive enzyme immunoassay as described previously (8).

RNA extraction and RT-qPCR. Total cellular RNA was extracted with TRIzol reagent (Life Technologies) according to the manufacturer's instructions. Quantification of cellular gene expression was performed by reverse transcription-quantitative PCR (RT-qPCR) using an Applied Biosystems 7500 fast real-time PCR system (Life Technologies) as described previously (47, 48). Primer/probe sets for qPCR targeting CKI-γ1, CKI-γ2, CKI-γ3, and TSSK2 genes were selected from validated Assays-on-Demand products (Life Technologies).

Intra- and extracellular infectivity assays. Intra- and extracellular infectivities of HCVcc were determined as described previously (8). The infectious titers were expressed as focus-forming units (FFU)/ml.

Cell viability assay. Cell viability was determined using the CellTiter-Glo luminescent cell viability assay (Promega) according to the manufacturer's instructions.

Expression of HCV proteins based on vaccinia virus, immunoprecipitation, immunoblotting, and silver staining. HCV protein expression based on vaccinia virus, immunoprecipitation, and immunoblotting were performed as previously described (8). pJFH1 was transfected into

– 325 –
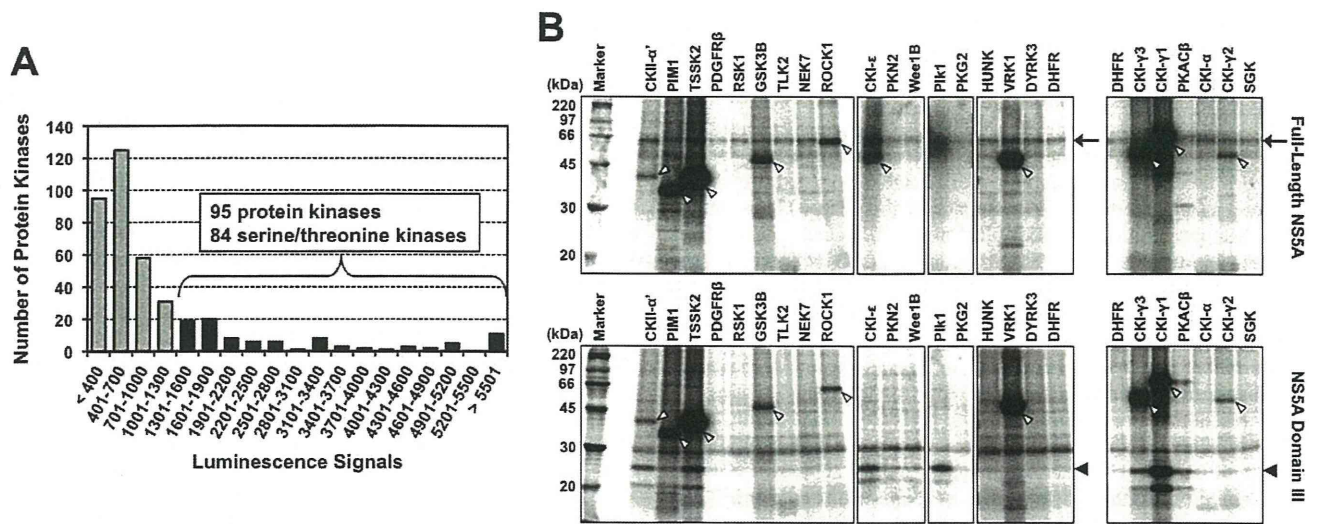
FIG 1 Identification of NS5A-associated kinases. (A) AlphaScreen-based protein-protein interaction assay. FLAG-tagged full-length NS5A, and each of 404 biotinylated human protein kinases, which were synthesized in a cell-free protein production system, were mixed with the detection mixture containing anti-FLAG antibody, protein A-conjugated acceptor beads, and streptavidin-coated donor beads in 384-well plates. Luminescence signals from the mixture were detected. Ninety-five protein kinases were identified with luminescence signals of ≥1,300, of which 84 were serine/threonine kinases. The assay was performed in duplicate for each sample, and data shown are mean values of duplicate experiments. (B) Exemplary autoradiographic images of NS5A phosphorylated *in vitro*. Purified kinases were mixed with biotinylated NS5A proteins coupled on streptavidin beads in kinase buffer containing [γ-^{32}P]ATP. After the reaction, samples were subjected to SDS-PAGE and autoradiography. The arrows, black arrowheads, and white arrowheads indicate phosphorylated full-length NS5A, phosphorylated NS5A domain III, and autophosphorylated kinases, respectively.

cells before infection with vaccinia virus expressing the T7 RNA polymerase. NS5A p58 and p56 protein levels were quantified by densitometry using Image J software. Silver staining of proteins in polyacrylamide gels was carried out using a Silver Stain MS kit (Wako Pure Chemical Industries, Osaka, Japan) in accordance with the manufacturer's protocol.

Subcellular fractionation analysis. Cells were suspended in homogenization buffer (10 mM HEPES-NaOH [pH 7.4], 0.25 M sucrose, and 1 mM EDTA) and disrupted by repeated passages through a 25-gauge needle. After low-speed centrifugation, postnuclear supernatants were layered on linear 11-ml iodixanol gradients from 2.5% to 30% and centrifuged at 40,000 rpm for 3 h in an SW41 rotor (Beckman, Fullerton, CA). Thirteen fractions (0.8 ml in each fraction) were collected from the top of the gradient. Each fraction was concentrated by ultrafiltration units with a 10-kDa molecular mass cutoff (Millipore, Bedford, MA), separated by SDS-PAGE, and immunoblotted with antibodies specific for NS5A, calnexin, and GM130.

Indirect immunofluorescence and microscopy analyses. Cells incubated for 3 days after infection with HCVcc of JFH-1 were fixed with 4% paraformaldehyde for 15 min at room temperature. After washing with PBS, the cells were permeabilized with 0.05% Triton X-100 in PBS for 15 min at room temperature and subsequently incubated in PBS containing 10% goat serum for 1 h. The cells were then costained with antibodies against core and NS5A, followed by incubation with fluorescent secondary antibodies. Cells were counterstained with Hoechst 33342 (Sigma-Aldrich) to label nuclei and BODIPY 493/503 (Life Technologies) to label lipid droplets and then mounted in Vectashield (Vector Laboratories, Burlingame, CA). Subcellular localization of HCV proteins was observed on a Leica SP2 AOBS laser scanning confocal microscope (Leica, Wetzlar, Germany). Colocalization of NS5A and LDs or core was evaluated quantitatively by using the intensity correlation analysis of the Image J software. To statistically compare degrees of colocalization, we determined the intensity correlation quotient (ICQ) (49). ICQ values are distributed between −0.5 and +0.5, with a value of ~0 reflecting random staining and values between 0 and +0.5 versus values between 0 and −0.5 indicative of dependent versus segregated immunolabeling, respectively.

Mass spectrometry analysis. Immunoprecipitated NS5A bands were excised from the gels after silver staining and destained, followed by in gel digestion with trypsin in 50 mM ammonium bicarbonate overnight at 30°C. Liquid chromatography-tandem mass spectrometry (LC-MS/MS) analysis was performed on an LTQ Orbitrap Velos hybrid mass spectrometer (Thermo Fisher Scientific, Bremen, Germany) using Xcalibur (version 2.0.7), coupled to an UltiMate 3000 LC system (Dionex LC Packings, Sunnyvale, CA). The Proteome Discoverer software (version 1.3; Thermo Fisher Scientific) was used to generate peak lists from the raw MS data files. The resulting peak lists were subsequently submitted to a Mascot search engine (version 2.4.1; Matrix Science, London, United Kingdom) and compared against the HCV protein sequences in the NCBI nonredundant protein database (version 20 January 2013; 74,0475 sequences) to identify peptides. The Mascot search parameters were as follows: two missed cleavages permitted in the trypsin digestion; variable modifications including oxidation of methionine, propionamidation of cysteine, and phosphorylation of serine, threonine, and tyrosine; peptide mass tolerance of ±5 ppm; fragment mass tolerance of ±0.5 Da. A minimum Mascot peptide score of 25 was set for peptide selection.

Statistical analyses. Statistical analyses were performed using the Student t test unless otherwise noted. A P level of <0.05 was considered significant.

RESULTS

A kinome-wide screening of human protein kinases for identification of NS5A-associated kinases. It has been reported that some protein kinases directly or stably associate with HCV NS5A and phosphorylate it *in vitro* (25, 50, 51). To search comprehensively to identify novel NS5A-associated kinases, a kinome-wide screening for interactions of full-length NS5A with human kinases was initially performed. We synthesized 404 human kinases with a wheat germ cell-free protein production system and screened them in terms of their association with NS5A by using a high-throughput assay system based on AlphaScreen technology (Fig. 1A;

– 326 –

TABLE 1 Serine/threonine kinases that exhibited efficient phosphorylation of NS5A

Kinase	LU	Relative kinase activity[a]	
		FL	D3
TSSK2	8,310	4.24	14.94
CKII-α′	5,068	2.30	8.20
Plk1	3,230	2.70	44.65
CKI-γ2	2,602	4.31	3.15
CKI-γ1	2,560	NA	138.69
CKI-γ3	2,218	0.23	52.51
CKI-ε	2,012	7.95	9.48
PKACβ	1,854	0.15	69.54
CKI-α	1,354	4.66	1.00

[a] LU, light units from the AlphaScreen; FL, full-length NS5A; D3, domain III of NS5A. NA, not assessed due to overlap between purified kinases and NS5A on the gel. The relative kinase activity is the fold increase of the *in vitro* activity of each kinase relative to that of DHFR.

see also Table S1 in the supplemental material). Ninety-five proteins were selected as those that possibly bind to NS5A under the cutoff condition of luminescence signals at ≥1,300. Among them, 84 were serine/threonine kinases, and Plk1 and CKII-α′, the catalytic subunit α′ of CKII whose associations with NS5A have been reported (25, 50), were found in the group as signals at 3,230 (Plk1) and 5,068 (CKII-α′). This suggested that our assay system is highly reliable for screening the NS5A-kinase interaction.

In vitro phosphorylation of NS5A by the identified NS5A binding serine/threonine was determined. Each kinase that was synthesized *in vitro* and purified was incubated with either full-length NS5A or domain III of NS5A in the presence of [γ-^{32}P]ATP and separated by SDS-PAGE. Phosphorylated NS5A proteins were then visualized by autoradiography (Fig. 1B). The relative kinase activity was determined by normalizing the band intensity of

phosphorylated NS5A with that of NS5A incubated with DHFR, which had no kinase activity and was used as a negative control. Twenty-nine out of 84 serine/threonine kinases were not accurately assessed due to their low levels of expression. As shown in Table 1, among a total of 55 kinases tested (see Table S2 in the supplemental material), nine (CKI-α, CKI-γ1, CKI-γ2, CKI-γ3, CKI-ε, CKII-α′, PKACβ, Plk1, and TSSK2) exhibited efficient phosphorylation of NS5A, defined as a more-than-4-fold or 8-fold increase in activity against the full-length NS5A or domain III of NS5A, respectively, compared to the negative control. Consistent with previous reports (9, 25, 50), Plk1 and CKII-α′ showed apparent kinase activities against NS5A *in vitro*.

Identification of an NS5A-associated kinase, CKI-α, that is important for the HCV life cycle. On the basis of the *in vitro* screenings, nine candidate kinases were further tested as to whether they play roles in the HCV life cycle. We conducted siRNA-based gene silencing of each kinase and assessed its effect on virion production. Huh7.5.1 cells were transfected with siRNAs targeting the kinases and infected with JFH-1 virus at an MOI of 1, 48 h after siRNA transfection. After an additional 72-h incubation, the viral core levels and infectious virus yields in cell culture supernatants were determined. Knockdown efficiencies of the targeted genes at 72 h after JFH-1 infection are shown in Fig. 2A. Efficient knockdown was confirmed either by immunoblotting or RT-qPCR. Figure 2B indicates the effects of gene silencing on virus production (upper panel) and on cell viability by ATP-based luminescence assays (lower panel). An approximately 30-fold reduction in infectious virus yields was observed following knockdown of ApoE, which has been shown to have important roles in HCV assembly and release (52). Among the kinases tested, silencing of CKI-α showed the most profound inhibition of infectious HCV production (~40-fold) without cytotoxicity. Knock down of CKII-α′ and PKACβ led to a moderate reduction in infectious virus pro-
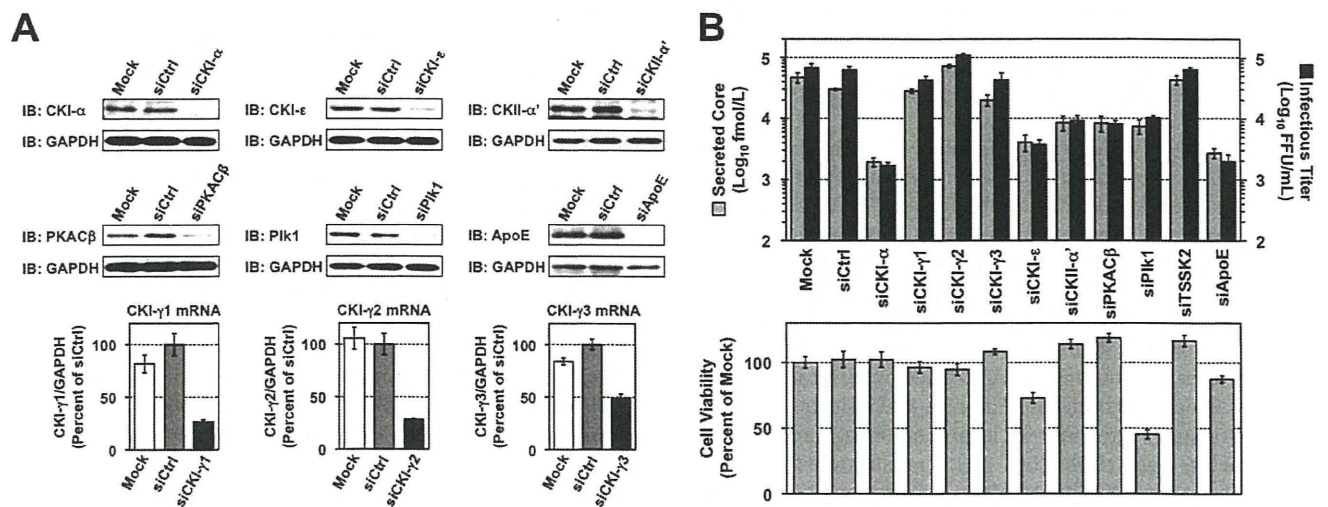

FIG 2 Identification of NS5A-associated kinases involved in the HCV life cycle. (A) siRNA-based gene silencing of NS5A-associated kinases. Huh7.5.1 cells were transfected with siRNAs targeting the indicated genes and were harvested 5 days later for immunoblotting (IB) and RT-qPCR to confirm knockdown efficiencies. mRNA levels of target genes relative to GAPDH mRNA were normalized with values for transfection of control siRNAs (siCtrl), which were set at 100%. Results represent the means ± standard deviations from three independent transfections of siRNA. Mock represents transfection without siRNA. (B) Infectious HCV production and cell viability following knockdown of NS5A-associated kinases. Huh7.5.1 cells were infected with JFH-1 virus at an MOI of 1, 2 days after siRNA transfection. Culture supernatants and cells were harvested 3 days later to determine infectious virus yields (upper panel) and cell viability (lower panel), respectively. Cell viability for each transfection was normalized to that for mock transfection (mock), which was set at 100%. Results shown represent the means ± standard deviations from three independent transfections of siRNA. Mock, transfection without siRNA.

– 327 –
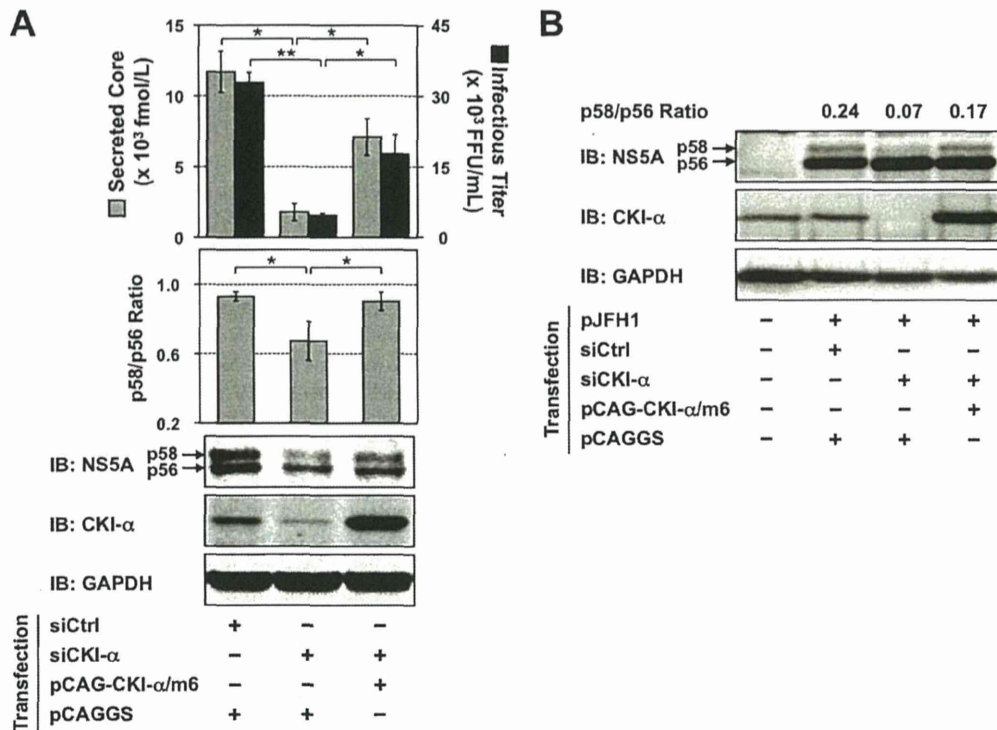
FIG 3 Restoration of NS5A hyperphosphorylation and infectious virus yields by ectopic expression of siRNA-resistant CKI-α. (A) Huh7.5.1 cells were cotransfected with the indicated siRNAs and plasmid DNAs. The next day, cells were infected with JFH-1 virus at an MOI of 0.5. Culture supernatants and cells were harvested an additional 3 days later for measurement of virus yields and immunoblotting (IB). The p58/p56 ratios were calculated after quantifying the band intensities of NS5A. Values shown represent the means ± standard deviations from three replicate experiments. *, $P < 0.05$; **, $P < 0.01$. (B) Huh-7 cells were transfected either with CKI-α siRNA (siCKI-α) or with an irrelevant control siRNA (siCtrl). The next day, cells were retransfected with pJFH1 and pCAG-CKI-α/m6 or empty vector (pCAGGS), followed by infection with vaccinia virus expressing the T7 RNA polymerase at an MOI of 10. NS5A bands were quantified by densitometric analysis, and the p58/p56 ratios were calculated. Immunoblotting images and values shown are representative of two independent experiments.

duction (~10-fold), which was consistent with previous reports showing that CKII-α′ and PKA are involved in virion assembly and viral entry, respectively (9, 53). Knockdown of CKI-ε and Plk1 also resulted in a moderate decrease in virion production (~20-fold), but they induced moderate to severe cell toxicity as well.

Thus, CKI-α, which phosphorylates NS5A, had the highest impact on HCV production based on *in vitro* comprehensive screenings for protein kinases and a subsequent siRNA-based assay.

To further demonstrate that impaired virus production results specifically from CKI-α silencing and is not an off-target effect of the siRNA, cells were cotransfected with CKI-α siRNA and a mutated CKI-α expression vector (pCAG-CKI-α/m6) that contained 6 base mismatches within the site targeted by the CKI-α siRNA without a change in amino acids, followed by JFH-1 infection at an MOI of 0.5 on the next day. The cells and culture supernatants were harvested 3 days later for immunoblotting and titrations of virus yields, respectively (Fig. 3A). Transfection of the CKI-α siRNA led to a significant reduction in infectious virus yields and in the p58/p56 ratio of NS5A. Ectopic expression of the siRNA-resistant CKI-α/m6 apparently restored virus yields ($P < 0.05$), as well as the p58/p56 ratio of NS5A ($P < 0.05$). Similar results regarding the p58/p56 ratio were obtained from immunoblot analysis following vaccinia virus-T7 polymerase-mediated expression of HCV proteins (Fig. 3B). These results indicated that impaired virion production and reduced NS5A hyperphosphorylation are

specifically caused by CKI-α silencing. Infectious virus yields showed a closer correlation with the p58/p56 ratio of NS5A than did the expression level of CKI-α, suggesting that the involvement of CKI-α in HCV production is through hyperphosphorylation of NS5A.

CKI-α is mainly involved in virion assembly in the HCV life cycle. Although it has been reported that CKI-α plays roles in the regulation of HCV RNA replication through NS5A phosphorylation, experiments addressing its involvement in the viral life cycle have been performed using the subgenomic replicon system (27). To determine the basic role of CKI-α in the production of infectious HCV, the effect of CKI-α silencing on individual steps in the HCV life cycle was assessed.

First, we used an HCVpp system to analyze viral entry. Two days after the siRNA transfection, the cells were infected with HCVpp derived from JFH-1 or VSV-Gpp and were cultured for a further 3 days (Fig. 4A). Consistent with a previous report (54), CLDN1 knockdown inhibited HCVpp entry by approximately 70%, but not VSV-Gpp entry, compared to transfection with negative control siRNA. CKI-α silencing did not affect HCVpp or VSV-Gpp entry, suggesting that CKI-α is not required for HCV entry.

Second, the effect of CKI-α knockdown was tested using an HCV subgenomic replicon system. Three days after the siRNA transfection, the cells were coelectroporated with the identical siRNA and JFH-1 subgenomic luciferase reporter replicon RNA,

– 328 –